in vivo *34*: 815-824 (2020)
doi:10.21873/invivo.11843

Surgical Ectrodactyly Repair Using Limb-lengthening and Bone Tissue Engineering Techniques in a Toy Dog Breed

MUN-IK LEE[1*], HO-HYUN KWAK[1*], JUN-HYUNG KIM[1], HYEOK-SOO SHIN[1], HEUNG-MYONG WOO[1] and BYUNG-JAE KANG[2]

[1]*Department of Veterinary Surgery, College of Veterinary Medicine and Institute of Veterinary Science, Kangwon National University, Chuncheon, Republic of Korea;*
[2]*Department of Veterinary Clinical Sciences, College of Veterinary Medicine and Research Institute for Veterinary Science, Seoul National University, Seoul, Republic of Korea*

Abstract. *Background/Aim: Bone tissue engineering is an emerging field of regenerative medicine that holds promise for the restoration of bones affected by trauma, neoplastic diseases, and congenital deformity. During the past decade, bone tissue engineering has evolved from the use of biomaterials that can only replace small areas of damaged bone, to the use of scaffolds in which grafts can be seeded before implantation. This case report proposes an alternative option for a veterinary patient suffering from ectrodactyly, which is one of several congenital deformities in dogs. A 2-month-old male toy poodle dog with ectrodactyly was treated using several stages of surgery involving pancarpal arthrodesis, limb lengthening, and bone tissue engineering techniques. Results and Conclusion: Over a period of 2 years, the operated limb gained almost the same function as the contralateral limb. Bone tissue engineering techniques can be used for the treatment of congenital deformities in dogs.*

Dysostoses are a group of congenital bone deformities arising from errors during embryonic development. Specific appendicular skeletal dysostoses include amelia, hemimelia, ectrodactyly, polydactyly, and syndactyly (1). Ectrodactyly (split-hand or lobster claw deformity) is an uncommon congenital malformation of the antebrachium, characterized by a soft tissue and boney split between metacarpal bones and the radius and ulna, along with deformities of the carpal bones (2).

In dogs, ectrodactyly has been reported in various breeds including the Dobermann Pinscher, Chow Chow, Cocker Spaniel, Irish Setter, Labrador Retriever, West Highland White Terrier, Siberian Husky, and crossbreeds (3-9). Although bilateral forelimb ectrodactyly has been reported in the literature (5, 10), it is predominantly a unilateral disease, affecting the first and second digits of the thoracic limbs in most cases. These conditions are present at birth, but lameness and deformity become more severe with age and more evident during loading. For this reason, clinical signs vary from mild deformity without lameness to severe deformity with non-weight bearing lameness (2). Radiographic findings in ectrodactyly are characterized by axial separation of the metacarpal and/or carpal bones, in which the cleft can reach up to the elbow joint, shortening of the affected limb, and luxation of the ipsilateral elbow (5).

Conservative treatment is a possible option for dogs with mild deformities or if the owner does not want to pursue a surgical procedure (2). Surgical management of ectrodactyly consists of amputation (11) or reconstruction methods. Reconstruction techniques may involve pancarpal arthrodesis, arthrodesis with ulna osteotomy or ostectomy, partial carpal arthrodesis, carpal and metacarpal stabilization with bone grafting, podoplasty, and ulnar lengthening (1, 3, 6, 8, 12, 13). The treatment option depends on the severity of the malformation. Furthermore, multiple surgical reconstructions may be needed.

In recent years, regenerative medicine approaches have been extensively investigated to improve cartilage and bone healing. Bone tissue engineering techniques are a new emerging field of regenerative medicine to treat congenital, neoplastic, acute traumatic, and sport-related skeletal injuries. Bone tissue engineering strategies involve the seeding of bone grafts onto a scaffold and the subsequent

*These Authors contributed equally to this study.

Correspondence to: Byung-Jae Kang, College of Veterinary Medicine, Seoul National University, 1 Gwanak-ro, Gwanak-gu, Seoul 08826, Republic of Korea. Tel: +82 28801248, e-mail: bjkang81@snu.ac.kr

Key Words: Bone tissue engineering, dog, ectrodactyly, limb lengthening, pancarpal arthrodesis.

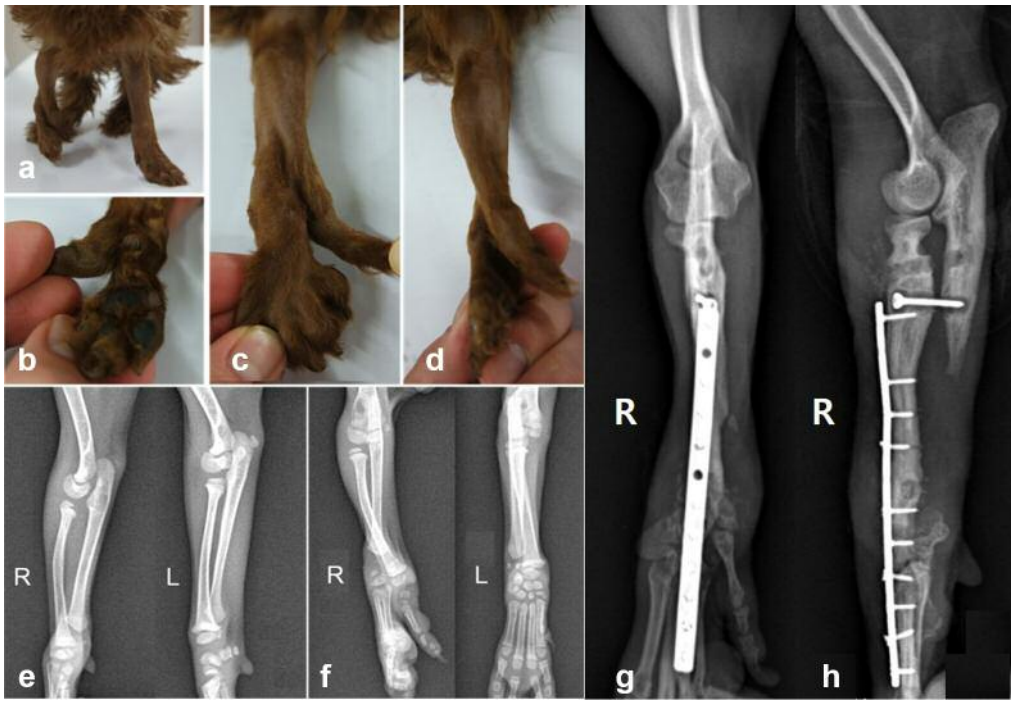

Figure 1. *Two-month-old male toy poodle with ectrodactyly of the right thoracic limb (a). Note the contracted metacarpal pad in the palmar view (b) and the cleft of the soft tissue between the first and second metacarpal bones (c, d). The lateral (e) and dorsoventral (f) radiographic views show that the carpal bones of right manus were hypoplastic and the associated elbow joint incongruity can be seen. The dorsoventral (g) and lateral (h) radiographic views are shown after right radial fracture fixation. R: Right; L: left.*

implantation of the construct *in vivo* to address a bone defect or a bone malformation.

In humans, many trials of treatments for congenital bony malformations, such as cleft palate and pseudarthrosis of the tibia, have been reported in pediatric patients (14, 15). However, in the veterinary literature, bone tissue engineering techniques are mainly focused, not on congenital deformities, but on the reconstruction of large bone defects caused by trauma or neoplastic diseases (16, 17).

The present case report describes a dog with an ectrodactyly deformity that received multiple stages of surgery, including pancarpal arthrodesis, limb lengthening, and bone tissue engineering techniques.

Case description. A 2-month-old male toy poodle presented with lameness and an associated congenital deformity of the right thoracic limb. On physical examination, the patient could not bear weight on his right forelimb and had a cleft between the first and second metacarpal bones, which was more evident under distraction of the first digit of the ipsilateral limb. The lesion extended to the whole metacarpal area proximally to the carpal joint and involved the metacarpal pad, which had an abnormal configuration (Figure 1a-d). The range of motion of the right elbow was limited and the laxity of the right carpal joint was also increased compared to the contralateral limb.

Radiographic examination revealed that a cleft existed between the first and second metacarpal bones and the right-sided ulnar carpal bone was missing. The right radius bowed to the medial direction and the overall length from the right antebrachium to the manus was shortened by approximately 15 mm compared to the left side (Figure 1e and f).

Based on the signalment of the patient, orthopedic examination, and radiological findings, ectrodactyly was diagnosed and a conservative management was performed with a splint for 3 months.

Surgical treatment section I and II. Four months after the first admission, the difference in length between the bilateral forelimbs was approximately 20 mm. The first surgical treatment was then performed in three phases, including pancarpal arthrodesis, ulnectomy, and podoplasty. A craniomedial skin incision was made from the distal one third of the radius to the third metacarpal bone. After separating the joints between the carpal bone and the soft tissues adjacent to the ulna, ostectomy of one third of the ulna was performed. Through a V-shaped skin incision between the first and second digits, the radius was separated from the first digit and

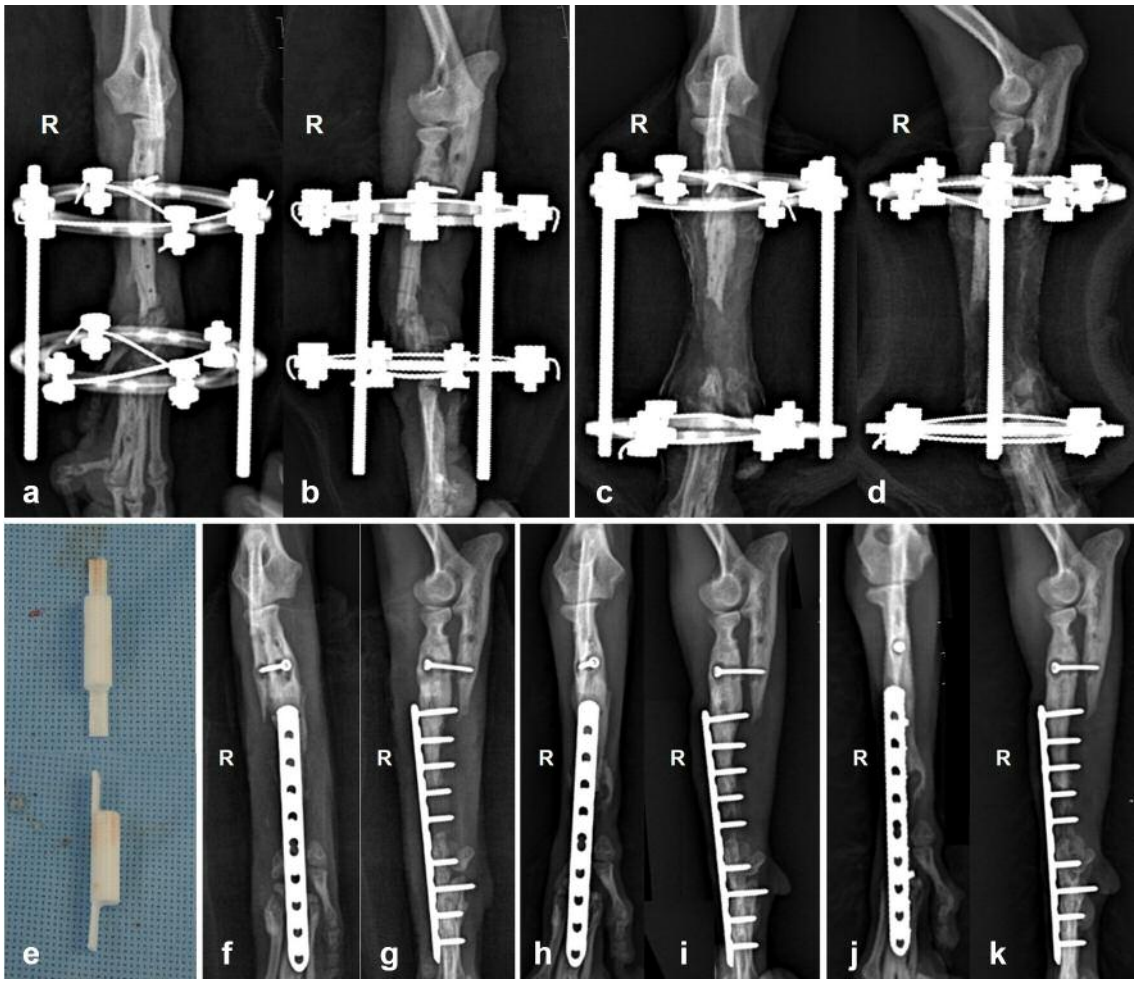

Figure 2. *Dorsoventral (a, c) and lateral (b, d) radiographic images before and after radial lengthening. The increased radial bone defect was fixed using a PCL/β-TCP 3D scaffold (e) and bone graft materials. Dorsoventral (f, h, j) and lateral (g, i, k) sequential orthogonal radiographs are shown at 2 weeks (f, g), 1 month (h, i), and 2 months (j, k) after radial defect fixation. R: Right.*

approximately 5 mm was excised for fusion with the intermedioradial carpal bone. A 1.2 mm T-shaped plate (IMEDICOM, Gunpo, Republic of Korea) with demineralized bone matrix (DBM; 0.1~0.5 mm, 1 ml; Veterinary Tissue Bank Ltd., Wrexham, UK) was applied after articulating the radius with the second, third, fourth, and fifth metacarpal bones and digits. Reconstruction of the soft tissues was achieved by overlapping the V-shaped skin incision between the first and second digits. The postoperative medications, tramadol (4 mg/kg, IV), meloxicam (0.2 mg/kg, IV) and cefazolin (25 mg/kg, IV) were injected and the patient was then prescribed cephalexin (25 mg/kg, PO, BID), tramadol (4 mg/kg, PO, BID), meloxicam (0.1 mg/kg, PO, SID), and famotidine (0.5 mg/kg, PO, BID) for 5 days.

One month following the first surgery, skin irritation due to the mobility of the right ulna was confirmed. To resolve the mobility of the right ulna, a radio-ulnar fixation was performed using two 1.5 mm cortical screws (IMEDICOM).

Three months after the pancarpal arthrodesis, implant failure and fracture of the right distal radius occurred due to a fight with another dog. A radial fracture fixation was performed using a 1.2 mm, 12-hole mini locking plate (IMEDICOM, Figure 1g and h). On physical examination at 1-month follow up, the patient used its right tiptoe in ambulation due to different lengths of the bilateral limbs.

Four months after radial fixation, implant failure occurred due to the owner's carelessness. A surgical plan was implemented, consisting of limb lengthening and fixation of the right radius to simultaneously resolve the difference in length of both forelimbs and the radial fracture (second surgery, 8 months after pancarpal arthrodesis). The gradational limb lengthening technique was performed to reduce the differences

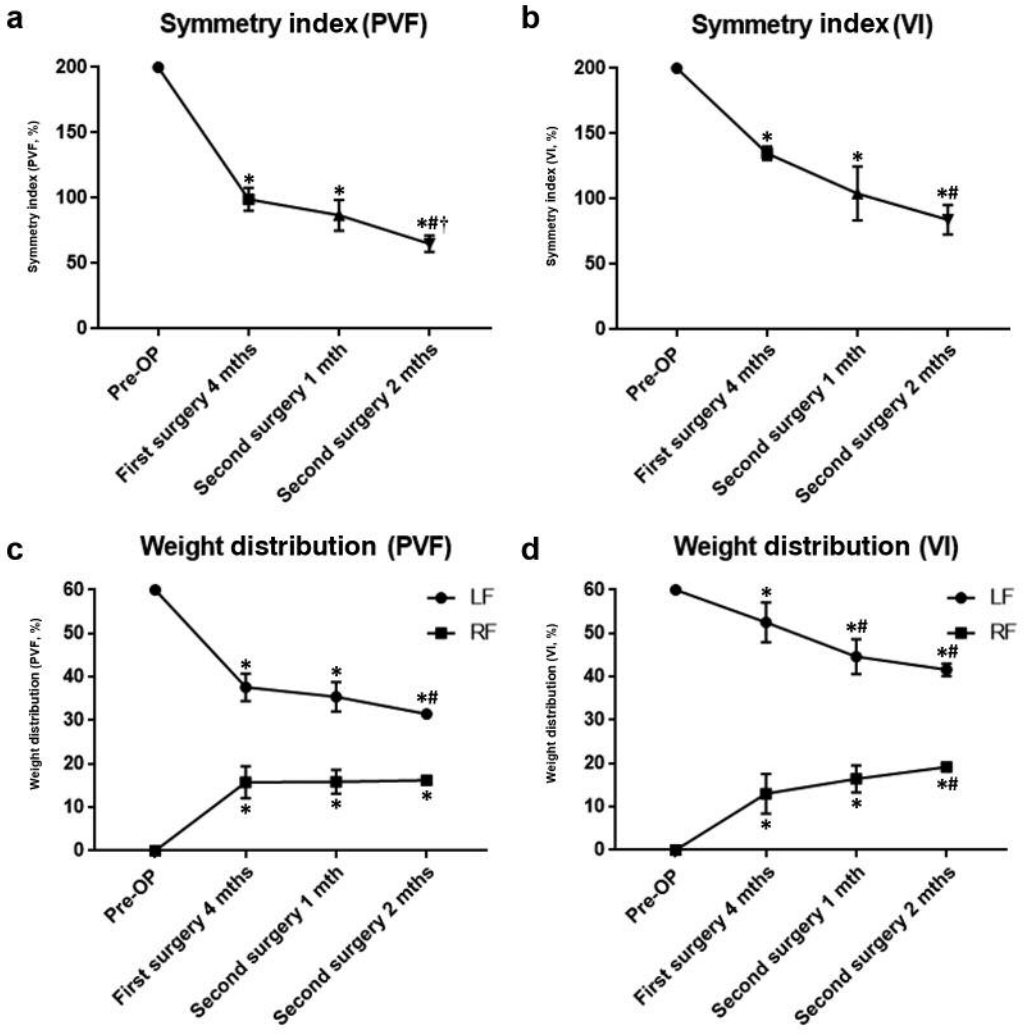

Figure 3. *Gait analysis on pressure sensor walkway. Symmetry index (a, b) of the bilateral forelimbs decreased after fixation of the PCL/β-TCP 3D scaffold to the radial bone defect. Weight distribution (c, d) at 1 and 2 months after the second surgery (limb lengthening and application of the PCL/β-TCP 3D scaffold) revealed a tendency to restore function of the right forelimb. PVF: Peak vertical force; VI: vertical impulse; RF: right forelimb; LF: left forelimb; *significant change from pre-operation; #significant change from 4 months after first surgery; †significant change from 1 month after second surgery.*

in the length of the bilateral forelimbs. A craniomedial skin incision was made from the proximal radius to the level of the distal metacarpal region. The previously inserted implants were removed and a mini circular external skeletal fixator (ESF; IMEX, Longview, TX, USA) assembled before the surgery was implanted using two Kirschner wires (K-wires) for the proximal fragment and four K-wires for the distal fragment (Figure 2a and b). The limb was lengthened at a rate of 1 mm per day for 20 days, as previously described (18). After terminating the distraction of the right forelimb, the length of the right forelimb was increased (Figure 2c and d).

Fixation of the right radius was performed using a 2.0 mm, 10-hole locking compression plate (LCP; Synthes, Warsaw, IN, USA) and a polycaprolactone (PCL)/β-tricalcium phosphate three-dimensional (3D) scaffold (T&R Mesh Plus; T&R Biofab, Seoul, Korea; Figure 3e), after 1 month of the distraction. A craniomedial skin incision was made from the proximal part of the right radius to the distal level of the third metacarpal region. After confirming the fractured gap of the radius and contouring the 3D scaffold, bone fragments were fixed with the 3D scaffold and plate. A bone graft mixture, consisting of recombinant human bone morphogenetic protein type 2 (rhBMP-2; 0.25 mg; NOVOSIS, Seongnam, Korea) and demineralized bone matrix (DBM; 0.1~0.5 mm, 1 ml; Veterinary Tissue Bank Ltd.), was used to cover the surgical site to expedite the bone healing process.

Surgical treatment section III. Four months after the application of the 3D scaffold, the patient presented with small masses at the site of the implants and showed intermittent non-weight-bearing lameness. The owner stated that they had been in a traffic accident 1 month earlier and that the patient had been in the car at the time of the accident. During a physical examination, three fistulas containing purulent exudate were found in the surgical area, which occurred due to inflammation caused by the mechanical instability of the implants. Radiographs showed the loosening of two screws applied to the plate at the fracture line of the right-sided distal diaphyseal radius. Based on the signalments of the patient, physical and orthopedic examination, and radiological findings, a nonviable defect nonunion fracture of the right-sided distal diaphyseal radius caused by implant failure was diagnosed.

To stabilize the inflammatory lesion, doxycycline (5 mg/kg, PO, BID) was applied, based on the antimicrobial sensitivity test, for 2 weeks and a strict restriction of exercise was indicated. The third surgery consisted of the application of a mini circular ESF with bone graft materials and plate fixation was performed following 2 weeks of stabilizing the inflammation. After removing the failed 3D implant and confirming that there was no bone marrow exposure in any of the segments, the bone marrow cavity was drilled with a 1.0 mm K-wire (Veterinary Instrumentation, Sheffield, UK). A mini circular ESF (IMEX) was applied to the proximal and distal segments of the fracture with four 1.0 mm K-wires for the proximal segment and two 1.0 mm K-wires for the distal segment. A mixture of bone grafts composed of cancellous chips (2~4 mm, Veterinary Tissue Bank Ltd.) and alginate microbeads loaded with rhBMP-2 (0.2 mg, NOVOSIS), as previously described (19), was applied to the defective area. A collagen sponge [1×2 cm; Lyostypt® (B-Braun, Barcelona, Spain)] wet with rhBMP-2 (0.05 mg, NOVOSIS), was used to encompass the surgical area. As time elapsed, radiographic images showed new bone formation in the bone defect (Figure 4a-d).

To improve the stability of the new bone adjacent to the proximal and distal fragments of the right radius and to avoid pin tract infection, plate fixation was performed 3 months after the application of the mini circular ESF. Before plate fixation, 3D reconstructions of computed tomography (CT) images were obtained after removing implants. These images showed that the new bone had connectivity with adjacent bone fragments. Based on the CT reconstruction images of the unaffected forelimb, a 3D printed bone model was extracted for contouring the plate (12 holes, 2.0 mm, LCP, Synthes). The plate was applied from the proximal diaphysis of the right radius to the level of the third metacarpal bone through a craniomedial skin incision.

After 2 months of follow-up, no major complications, such as fractures of the bone or implant, were found, except for the loosening of the screw in the most proximal hole of the plate. The loosened screw was removed and tested for microbial contamination. At the follow-up examination 7 months after plate application, a skin irritation was observed, caused by excessive tension force on the region of the implant. To avoid infection through the skin lesion, the implants were removed.

Results

Surgical treatment sections I and II. Two months after the application of the 3D implant, the patient showed an improved gait pattern, showing weight-bearing on his right forelimb without complications and was expected to have improved ambulation. The difference in length between the bilateral limbs at this time was only 10 mm. Radiologically, the apparatus and alignment of the implants were good for 2 months after the correction and new bone was formed at the scaffold application site (Figure 2f-k). Symmetry index and weight distribution were measured on a pressure sensor walkway and data were analyzed using a repeated measures ANOVA, with a post hoc Sidak multiple comparisons test. Gait analysis showed that the degree of asymmetry was restored to some extent during the 2 months of follow-up after the second surgery (Figure 3a and b). Weight distribution analysis showed that the right forelimb ratio was increased and that the weight distribution of the affected limb increased to 60% of the normal limb (Figure 3c and d). The owner was satisfied and the quality of life of the patient was increased because amputation was avoided.

Surgical treatment section III. Radiographic examination during the follow-up period showed that the fracture line was restored and the opacity of the bone grafts increased (Figure 4e-j). CT examination was also performed after implant removal to evaluate bone properties compared to the left radius. Based on 3D reconstruction images of the patient's normal radius and surgically treated radius, Hounsfield unit (HU) values were measured in randomly selected regions of the affected leg where the bone graft was implanted. In the normal radius, HU measurements were made at the same level as the affected radius (Figure 5a). The HU values of the affected and unaffected forelimbs were then compared using a Student's *t*-test. The HU values of the normal bone tissue did not differ from the HU values of the site where the bone grafts were inserted (Figure 5b). Furthermore, the patient showed improved ambulation during the follow-up period and gait analysis revealed that the differences in peak vertical force and vertical impulse between the bilateral forelimbs decreased (Figure 5c and 5d). After the third surgical treatment, symmetry index and weight distribution were again measured on a pressure sensor walkway and analyzed using

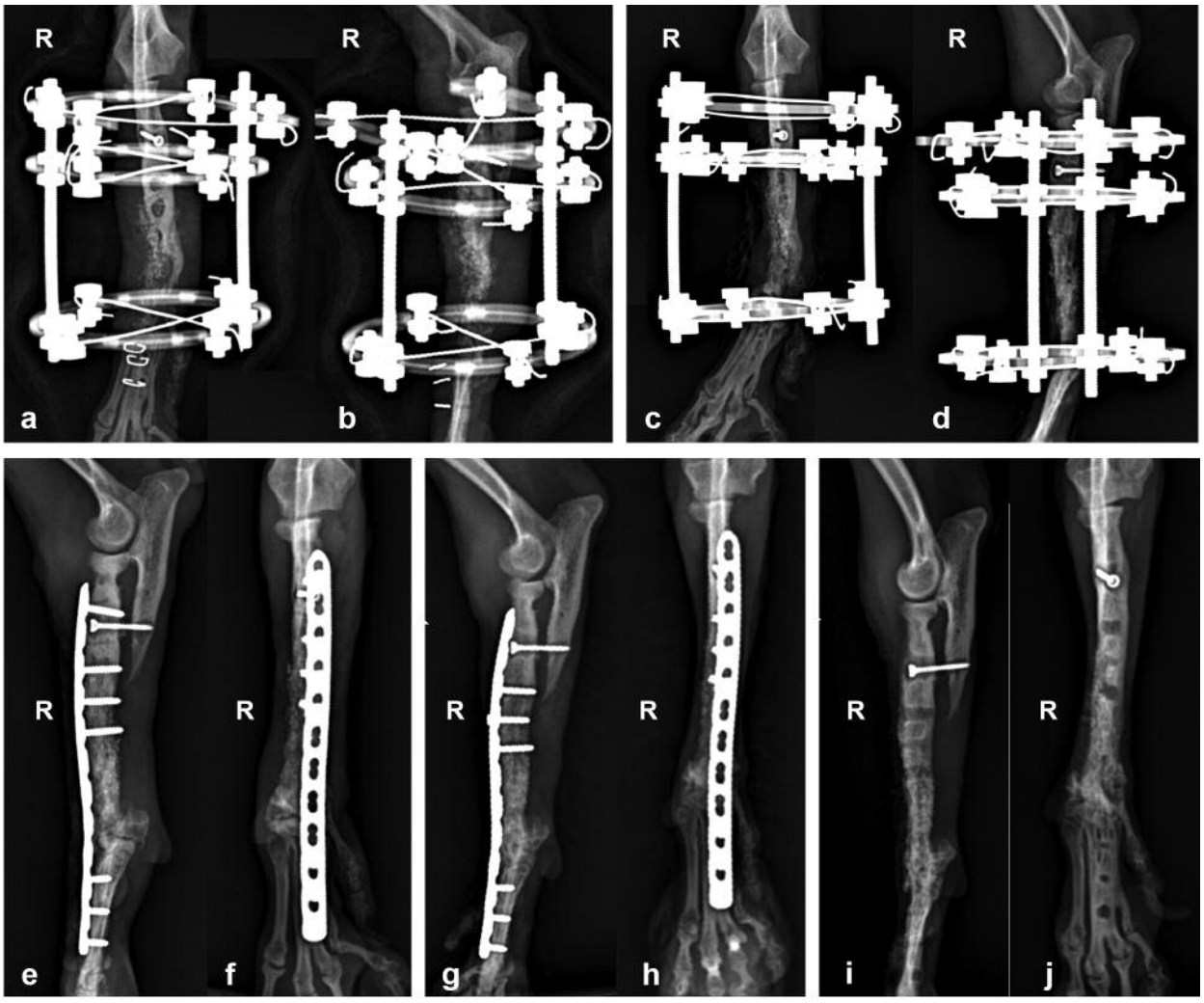

Figure 4. *Serial orthogonal radiographs at 0 days (a, b) and 3 months (c, d) after fixation of the mini circular ESF with bone graft materials. New bone formation was confirmed by increased radio-opacity in the bone grafting region. Sequential radiographic images are shown at 2 weeks (e, f), 2 months (g, h), and 8 months (1 month after plate removal; i, j) after plate fixation. After the removal of plate due to a skin irritation, the fracture line in the distal radial region is not observed and the radio-opacity of the new bone is further increased compared to 3 months after the application of the mini circular ESF and bone grafts. a, c, e, g, i: Dorsoventral views; b, d, f, h, j: lateral views; R: right.*

a repeated measures ANOVA with a post hoc Sidak multiple comparisons test. The weight distribution of the right forelimb also increased 1 month after plate removal. The weight distribution of the treated limb was found to increase to the level of 70% of the normal limb (Figure 5e and 5f).

A longer follow-up was not performed due to the owner's condition. However, at 10 and 12 months postoperatively, phone calls with the owner revealed that the result of the treatment was very satisfactory and that the patient was well and without pain or marked lameness on the operated leg.

Discussion

There are several different therapeutic options to treat ectrodactyly and the choice of treatment depends on the type and severity of the malformation. As a consequence, every case should be carefully evaluated to determine the most appropriate treatment, considering also that the literature regarding the management of this abnormality consists of only a few case reports (20). In our case, the patient was using a splint for 1 month, but the function of the right forelimb was unacceptable and further surgical treatment was considered. For this reason, pancarpal arthrodesis and

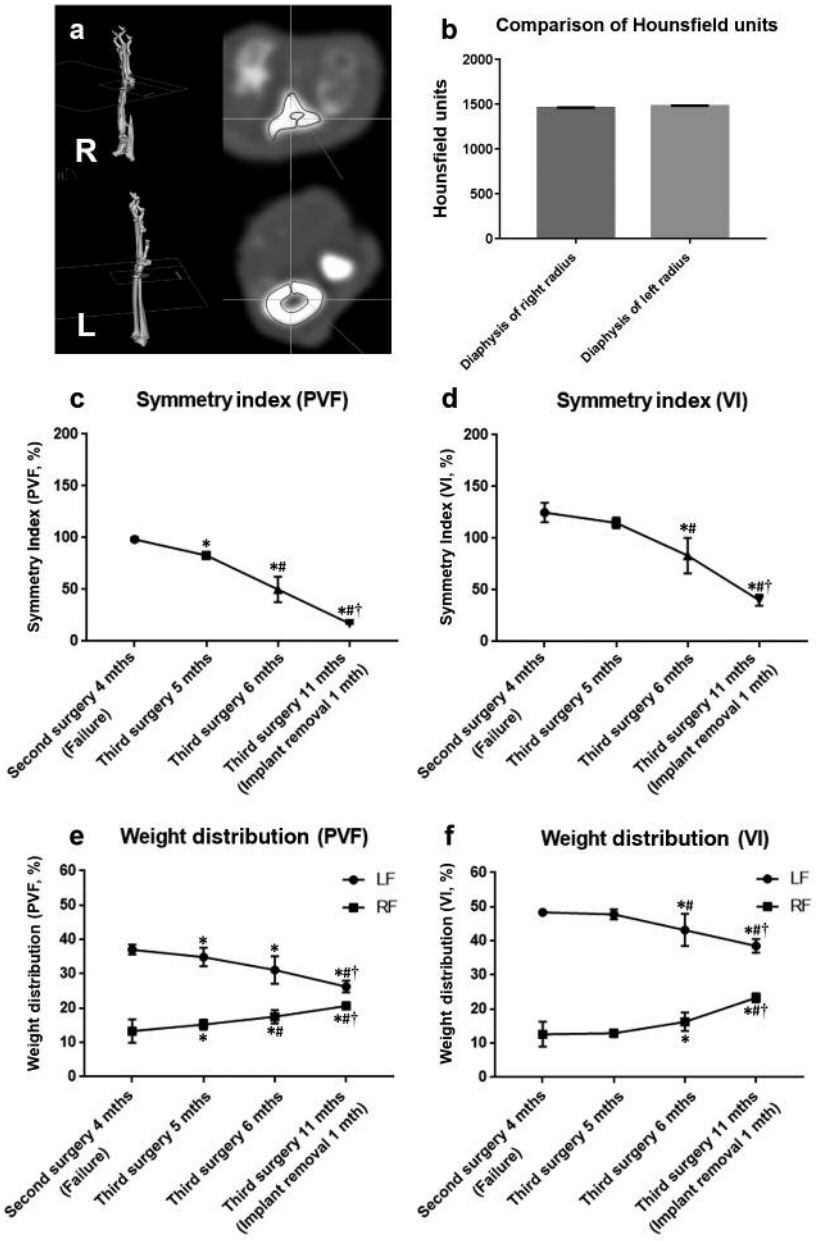

Figure 5. *Measurement of HU values based on five randomly selected regions of the right and left radius from CT reconstruction images (a). No significant difference between bilateral radii is observed (b). Gait analysis on pressure sensor walkway (c-f). Symmetry index (c, d) of the bilateral forelimbs decreased after application of a mini-circular ESF and bone graft materials. Analysis of weight distribution (e, f) at 5, 6, and 8 months after the third surgery (bone grafting and plate fixation) revealed a tendency to restore the function of the right forelimb. PVF: Peak vertical force; VI: vertical impulse; R: right; L: left; *significant change from 4 months after second surgery; #significant change from 5 months after third surgery; †significant change from 6 months after third surgery.*

podoplasty were performed for soft tissue reconstruction at an early age. Because of the reconstruction of soft tissue between the first and second digits, a favorable result was achieved in the immediate postoperative period, with a satisfactory functional recovery of the metacarpal pads, which are essential for bearing the weight of the manus. As reported in a previous study, traumatic damage to the web tissue between the toes of a normal dog (split web) can result in some lameness due to loss of support of the toes adjacent to the injury (21). Thus, the rationale behind the fusion of

the cleft, used to treat the case described here, was to provide this support. Furthermore, it was thought that the fusion between the metacarpal pad and the second digital pad would have provided functional support after performing limb lengthening and bone tissue engineering techniques.

In recent decades, bone tissue engineering techniques, such as limb salvage procedures, have been used to treat critical-sized bone defects in veterinary patients (17, 22-24). Some studies have demonstrated the effectiveness of BMP-2 alone, or in combination with scaffolds, in inducing bone formation and healing of long bone defects (17, 19, 22-25). In the present case, an implant failure occurred 3 months after arthrodesis and the patient received an implant replacement, which also failed 4 months after application. There was no additional option for treating the affected limb, except amputation, which is only treatment previously reported for ectrodactyly (1, 3, 6, 12, 13, 26). However, the owner was eager to preserve the patient's limb and therefore, we attempted limb-sparing surgery using a limb lengthening technique to compensate for the difference in length between the bilateral forelimbs and bone tissue engineering techniques as part of the final treatment.

The current case demonstrates that ectrodactyly in dogs can be repaired using various bone graft materials, such as rhBMP-2 and DBM, combined with a PCL/β-TCP 3D scaffold, to promote bone healing activity in the lengthened gap and the radial bone defect. Similar to a previous study showing that a PCL/β-TCP scaffold implanted in a canine mandibular defect model showed new bone formation 8 weeks after implantation (27), new bone formation in the current case was confirmed, based on radiographic evaluation, 2 months after PCL/β-TCP 3D scaffold implantation. Furthermore, Choi *et al*. reported that a PCL/β-TCP 3D scaffold applied in a canine patient with a radial bone defect caused by osteosarcoma, showed connectivity with adjacent bone tissue (17). However, the same study highlighted the importance of fast osteoinduction and osteointegration when using a PCL/β-TCP scaffold in a weight-bearing region, such as the long bone (17). Bina *et al*. reported that using the PCL/β-TCP scaffold with platelet-rich plasma in a critical-sized femoral defect in rats, resulted in successful bone healing, according to histological and biomechanical evaluation (25). In the present case, we used a PCL/β-TCP scaffold with rhBMP-2 and DBM for bone regeneration of the affected limb, resulting in early new bone formation, as seen in radiographic and kinetic evaluation (Figure 2 and 3). However, the patient was involved in a car accident and as a result, the implant failed once again. Although the patient could bear his weight using the right forelimb 2 months after PCL/β-TCP scaffold implantation, based on radiographic evaluation at the time of implant failure, bone density was low and the PCL/β-TCP scaffold was not connected to the adjacent bone fragments. According to previous studies, when using a PCL/β-TCP scaffold in long bones to which a weight-bearing force is applied, there is possibility that the scaffold may fracture before osteointegration is fully completed (17). Moreover, in the present case, it was thought that the PCL/β-TCP scaffold could no longer play a role in bone regeneration due to a massive trauma from a car accident. Therefore, the treatment using the PCL/β-TCP scaffold was considered to have failed and a more stable fixation with faster bone-healing activity was required to treat the radial bone defect.

The third surgical treatment focused on correction of the radial non-union defect. Paley reported that the tensioned wires of the circular ESF immobilize bone segments and adequately resist bending, shearing, and torsional forces, while allowing axial micromotion at the osteotomy fracture site (28). Axial micromotion is also thought to be important in creating a mechanical environment conducive for osteogenesis and is thought to enhance fracture healing (29). Piras *et al*. also reported that circular ESFs may be more effective at restoring blood supply than bone plates in toy breed dogs (30). In the present case, it is thought that the circular ESF provided bone grafts with a suitable biological and biomechanical environment to generate new bone in the radial bone defect. Furthermore, by using the circular ESF, the length of the right antebrachium could be restored. For these reasons, the use of circular ESFs can be an effective method to treat large bone defects in toy breed dogs.

The releasing profile of BMP-2 is one of the most important factors affecting bone regeneration. It has been shown that a burst of BMP-2 release within the first few days, followed by a sustained release, is essential for improving the osteoinductive activity of BMP-2 (31). According to an *in vivo* study in a rat carvarial defect model, the use of alginate microbeads as carriers of BMP-2, results in a burst release pattern within the first few days, followed by a long-term sustained release pattern. Furthermore, the same study also found that rats implanted with BMP-2-loaded alginate microbeads showed more effective bone formation, when compared to other experimental groups (19). Collagen sponges, which show a sustained release pattern, are also routinely used as carriers of BMP-2. Faria *et al*. reported that an rhBMP-2-loaded absorbable collagen sponge resulted in better bone-healing activity and functional recovery in a canine tibial osteotomy model than treatment with only rhBMP-2, as evidenced by force plate and radiographic evaluation (32). In the present case, rhBMP-2-loaded alginate microbeads and a collagen sponge were implanted at the same time. Based on radiographic examination, new bone formation was observed earlier than with the former treatment using a PCL/β-TCP scaffold. This may be due to the synergistic effect of the collagen sponge and alginate microbeads. The current results suggest that the use of alginate microbeads and collagen sponges as carriers may be an effective method for maximizing the

osteoinductive properties of rhBMP-2 in critical-sized bone defects in veterinary patients. Moreover, as described in the current case, these kinds of approaches using bone tissue engineering techniques can be used as alternatives for treating large bone defects caused by traumatic or neoplastic diseases, as well as congenital limb deformities.

Despite the completion of the patient's growth, a large difference in length between bilateral forelimbs was not observed. Furthermore, the affected limb had almost the same HU value as the contralateral limb following CT examination (Figure 5) and the patient could bear his weight with the right forelimb. However, gait analysis showed that the weight distribution of the affected limb did not increase to same level as the normal limb after the second and third surgical treatments (Figure 2 and 5c, d). Carpal flexion is known to be naturally eliminated in dogs with pancarpal arthrodesis (33). A previous study also described that propulsive forces and vertical impulses are significantly lower in dogs that have undergone pancarpal arthrodesis than in normal dogs (33). Furthermore, the patient in this case underwent multiple surgical treatments from a young age, which may have resulted in fibrosis of the right carpal joint and the surrounding tissue. For these reasons, the full function of the right forelimb could not be recovered. However, by obtaining satisfactory function, the quality of life of the patient could be improved.

Unlike previous methods used to treat ectrodactyly, the patient in this case report was able to obtain a newly formed right forelimb, instead of undergoing amputation, which is the standard treatment in such cases. Furthermore, no major complications were observed after several surgical treatments. However, these procedures were only performed in one case and a bone biopsy procedure was not performed to analyze the new bone compared to normal bone structure and assess the possibility of refracture. Furthermore, a longer period of follow-up is needed to monitor changes in the new bone tissue and perform a functional evaluation of the treated limb.

In conclusion, to the best of our knowledge, this is the first attempt to treat ectrodactyly using limb lengthening and bone tissue engineering techniques in a veterinary patient. These technologies are feasible treatment methods for congenital deformities, tumors of the extremities, and large bone defects caused by trauma.

Conflicts of Interest

The Authors declare that there are no conflicts of interest regarding this study.

Authors' Contributions

MIL, HHK and BJK conceived the case study and performed its design and coordination. MIL, HHK, JHK and HSS performed the experiment and conducted data analysis. BJK participated in data analysis and interpretation. HHK, HMW and BJK proofread the manuscript and gave final approval of the version to be published. All Authors read and approved the final manuscript.

Acknowledgements

This study was supported by the Basic Science Research Program through the National Research Foundation of Korea (NRF), funded by the Ministry of Education (No. 2018R1D1A1B07047451).

References

1 Towle HA and Breur GJ: Dysostoses of the canine and feline appendicular skeleton. J Am Vet Med Assoc *225(11)*: 1685-1692, 2004. PMID: 15626218. DOI: 10.2460/javma.2004.225.1685

2 Towle HA, Breur GJ and Tobias KM: Veterinary surgery small animal. 2nd ed. Saint Louis, Elsevier Saunders, pp. 1112-1126, 2018.

3 Barrand K: Ectrodactyly in a West Highland white terrier. J Small Anim Pract *45(6)*: 315-318, 2004. PMID: 15206479. DOI: 10.1111/j.1748-5827.2004.tb00243.x

4 Bingel SA and Riser WH: Congenital elbow luxation in the dog. J Small Anim Pract *18(7)*: 445-456, 1977. PMID: 560607. DOI: 10.1111/j.1748-5827.1977.tb05911.x

5 Carrig C, Wortman J, Morris E, Blevins W, Root C and Hanlon G: Ectrodactyly (split-hand deformity) in the dog. Vet Radiol *22(3)*: 123-144, 1981. DOI: 10.1111/j.1740-8261.1981.tb01363.x|

6 Frey M and Williams J: What is your diagnosis? Radiographic diagnosis-ectrodactyly. J Am Vet Med Assoc *206(5)*: 619-620, 1995. PMID: 7744678.

7 Harasen G: Surgical management of ectrodactyly in a Siberian husky. Can Vet J *51(4)*: 421-424, 2010. PMID: 20592835.

8 Milton J and Montgomery R: Congenital elbow dislocations. Vet Clin N Am: Small Anim Pract *17(4)*: 873-888, 1987. PMID: 3303632. DOI: 10.1016/s0195-5616(87)50082-1

9 Poletto Ferreira M, Meller Alievi M, dos Santos Dal-Bó I, Silveira Nóbrega F, Sieczkowski Gonzalez PC, de Castro Beck and Carlos Afonso: Surgical management of ectrodactyly in a dog. Semina: Ciênc Agrár *37(2)*: 891-896, 2016. DOI: 10.5433/1679-0359.2016v37n2p891

10 Carvallo FR, Dominguez AS and Morales PC: Bilateral ectrodactyly and spinal deformation in a mixed-breed dog. Can Vet J *52(1)*: 47-49, 2011. PMID: 21461206.

11 Di Dona F, Della Valle G, Meomartino L, Lamagna F and Fatone G: Congenital deformity of the distal extremities in three dogs. Open Vet J *6(3)*: 228-233, 2016. PMID: 27928521. DOI: 10.4314/ovj.v6i3.11

12 Innes J, McKee W, Mitchell R, Lascelles B and Johnson K: Surgical reconstruction of ectrodactyly deformity in four dogs. Vet Comp Orthop Traumatol *14(4)*: 201-209, 2001. PMID: 22058371. DOI: 10.5326/JAAHA-MS-5609

13 Murray JH and Fitch RD: Distraction histiogenesis; principles and indications. J Am Acad Orthop Surg *4(6)*: 317-327, 1996. PMID: 10797199. DOI: 10.5435/00124635-199611000-00004

14 Panetta NJ, Gupta DM, Slater BJ, Kwan MD, Liu KJ and Longaker MT: Tissue engineering in cleft palate and other congenital malformations. Pediatr Res *63(5)*: 545, 2008. PMID: 18427300. DOI: 10.1203/PDR.0b013e31816a743e

15 Richards BS and Anderson TD: rhBMP-2 and intramedullary fixation in congenital pseudarthrosis of the tibia. J Pediatr

Orthop *38(4)*: 230-238, 2018. PMID: 27261960. DOI: 10.1097/BPO.0000000000000789

16 Massie AM, Kapatkin AS, Fuller MC, Verstraete FJ and Arzi B: Outcome of nonunion fractures in dogs treated with fixation, compression resistant matrix, and recombinant human bone morphogenetic protein-2. Vet Comp Orthop Traumatol *30(2)*: 153-159, 2017. PMID: 28094415. DOI: 10.3415/VCOT-16-05-0082

17 Choi S, Oh Y, Park K, Lee J, Shim J and Kang B: New clinical application of three-dimensional-printed polycaprolactone/β-tricalcium phosphate scaffold as an alternative to allograft bone for limb-sparing surgery in a dog with distal radial osteosarcoma. J Vet Med Sci *81(3)*: 434-439, 2019. PMID: 30662043. DOI: 10.1292/jvms.18-0158

18 Coutin JV, Lewis DD, Kim SE and Reese DJ: Bifocal femoral deformity correction and lengthening using a circular fixator construct in a dog. J Am Anim Hosp Assoc *49(3)*: 216-223, 2013. PMID: 23535751. DOI: 10.5326/JAAHA-MS-5836

19 Lee YH, Lee B, Jung YC, Yoon B, Woo H and Kang B: Application of alginate microbeads as a carrier of bone morphogenetic protein-2 for bone regeneration. J Biomed Mater Res B *107(2)*: 286-294, 2019. PMID: 29569344. DOI: 10.1002/jbm.b.34119

20 Pisoni L, Del Magno S, Cinti F, Dalpozzo B, Bellei E and Cloriti E: Surgical induction of metacarpal synostosis for treatment of ectrodactyly in a dog. Vet Comp Orthop Traumatol *27*: 166-171, 2014. PMID: 24569849. DOI: 10.3415/VCOT-13-01-0019

21 Denny HR and Butterworth SJ: A guide to canine and feline orthopaedic surgery 4th ed. Oxford, Blackwell Science, pp. 431, 2000.

22 Heckman JD, Boyan BD, Aufdemorte TB and Abbott JT: The use of bone morphogenetic protein in the treatment of non-union in a canine model. J Bone Joint Surg Am *73(5)*: 750-764, 1991. PMID: 2045401.

23 Sciadini MF, Dawson JM, Johnson KD and Sciadini M: Evaluation of bovine-derived bone protein with a natural coral carrier as a bone-graft substitute in a canine segmental defect model. J Orthop Res *15(6)*: 844-857, 1997. PMID: 9497809. DOI: 10.1002/jor.1100150609

24 Sciadini MF and Johnson KD: Evaluation of recombinant human bone morphogenetic protein-2 as a bone-graft substitute in a canine segmental defect model. J Orthop Res *18(2)*: 289-302, 2000. PMID: 10815831. DOI: 10.1002/jor.1100180218

25 Rai B, Oest ME, Dupont KM, Ho KH, Teoh SH and Guldberg RE: Combination of platelet-rich plasma with polycaprolactone-tricalcium phosphate scaffolds for segmental bone defect repair. J Biomed Mat Res A *81(4)*: 888-899, 2007. PMID: 17236215. DOI: 10.1002/jbm.a.31142

26 Milton J and Montgomery R: Congenital elbow dislocations. Vet Clin N Am Small Anim Pract *17(4)*: 873-888, 1987. PMID: 3303632. DOI: 10.1016/s0195-5616(87)50082-1

27 Shim J, Won J, Park J, Bae J, Ahn G and Kim C: Effects of 3D-printed polycaprolactone/β-tricalcium phosphate membranes on guided bone regeneration. Int J Mol Sci *18(5)*: 899, 2017. PMID: 28441338. DOI: 10.3390/ijms18050899

28 Paley D: Operative principles of Illizarov. 1st ed. Milian, Springer, pp. 31-41, 1991.

29 Welch RD and Lewis DD: Distraction osteogenesis. Vet Clin North Am Small Anim Pract *29(5)*: 1187-1205, 1999. PMID: 10503291. DOI: 10.1016/s0195-5616(99)50109-5

30 Piras L, Cappellari F, Peirone B and Ferretti A: Treatment of fractures of the distal radius and ulna in toy breed dogs with circular external skeletal fixation; a retrospective study. Vet Comp Orthop Traumatol *24(3)*: 228-235, 2011. PMID: 21373718. DOI: 10.3415/VCOT-10-06-0089

31 Li A, Bennett D, Gibbs C, Carmichael S, Gibson N and Owen M: Radial carpal bone fractures in 15 dogs. J Small Anim Pract *41(2)*: 74-79, 2000. PMID: 10701191. DOI: 10.1111/j.1748-5827.2000.tb03167.x

32 Faria ML, Lu Y, Heaney K, Uthamanthil RK, Muir P and Markel MD: Recombinant human bone morphogenetic protein-2 in absorbable collagen sponge enhances bone healing of tibial osteotomies in dogs. Vet Surg *36(2)*: 122-131, 2007. PMID: 17335419. DOI: 10.1111/j.1532-950X.2007.00242.x

33 Andreoni A, Rytz U, Vannini R and Voss K: Ground reaction force profiles after partial and pancarpal arthrodesis in dogs. Vet Comp Orthop Traumatol *23(1)*: 1, 2010. PMID: 19997672. DOI: 10.3415/VCOT-09-03-0030

Received October 30, 2019
Revised November 5, 2019
Accepted November 12, 2019